Three Phase three level controlled Bidirectional ac-dc converter with Bidirectional Dual Active bridge isolated Converter system

April 22, 2022

Ashish Meena(214102110)-DAB
Deepak Kumar (214102111)-Charging
Cilaveni Satish Chandra(216102008)-NPC

Objective

Design an electric vehicle battery charging system. The battery charging system consists of two converter system one AC-DC converter and another one as DC-DC converter.

Specifications

Input voltage : Three phase 3.3 kV (50 Hz)
Battery details: 400 V, 70 kWhr
Battery charging Time (20-80 SOC) : 1.5 hr
Input power factor = 1, Input current THD = 5%
Output voltage ripple for ac-dc converter = 5%

Block Diagram of the EV charging system

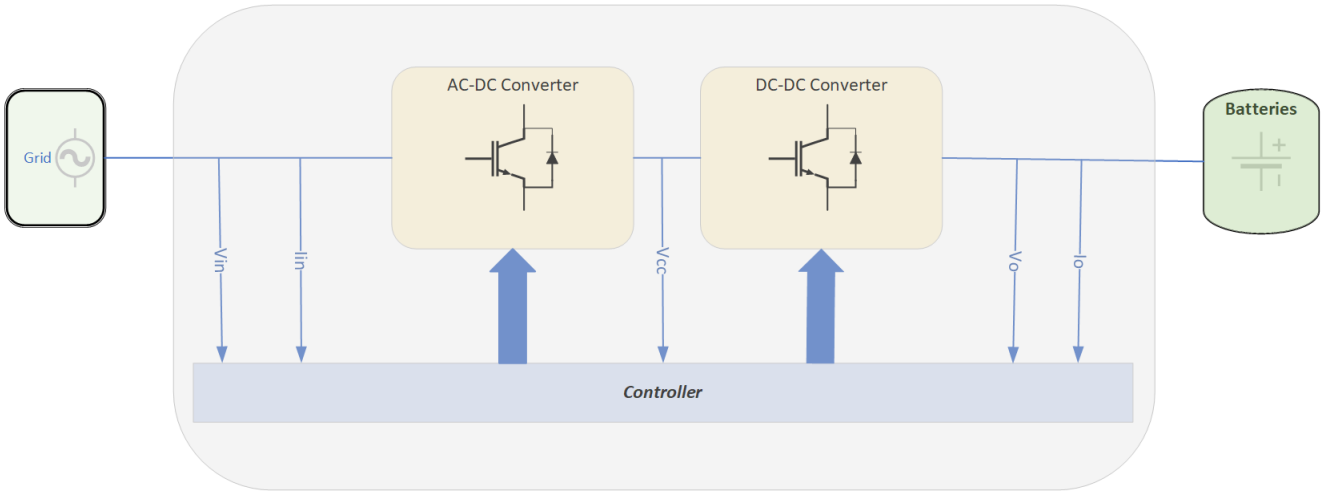

Figure 1: Block Diagram

Design Procedure

1 AC-DC Converter Design

1.1 Power Circuit Design

The power circuit of the AC-DC converter system is shown in Fig. 2.We use Neutral Point Clamped (NPC) AC-DC converter as a 3-Level AC-DC converter which is connected to the three-phase grid through L-filter.
The value of filter inductance is calculated as

$$L_f = \frac{v_{dc}}{4 * \triangle f_{sw} * \triangle I_{max}}$$

$$L_f = 14mH$$

The output capacitance of DC link is calculated as

$$C_{dc} = \frac{2 * \triangle t * \triangle P_{max}}{V_{dc} - (V_{dc} - \triangle V_{dcl})^2}$$

$$C_{dc} = 0.3mF$$

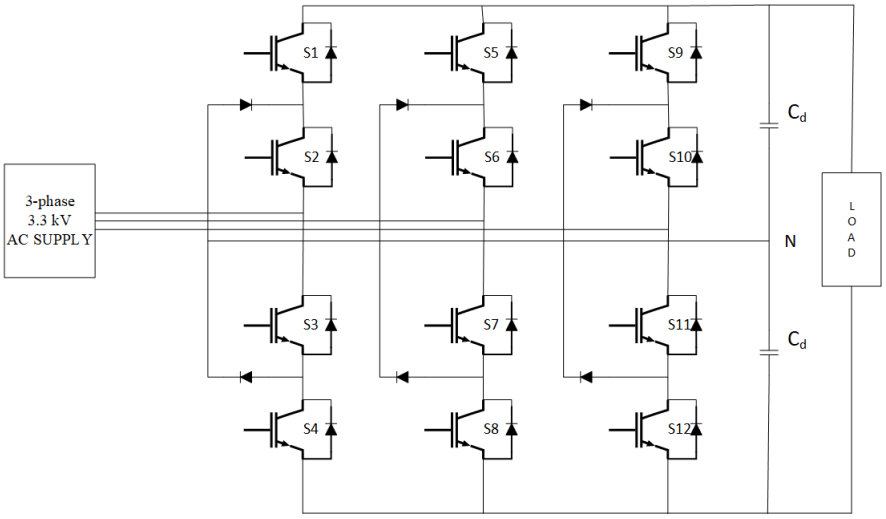

Figure 2: Circuit Diagram of AC-DC NPC Converter

The converter is designed for 30 kVA. For the standard three-phase, 50-Hz grid voltage of 3.3 kV, a load of 30 kW at 6.4 kV dc bus voltage. Below this power level, the effect of lower order harmonics becomes significant. Table 1 summarizes the system parameters considered for the analysis including the voltage and power ranges.

Parameter	Value
MV grid voltage	3.3 kV
DC bus voltage	6.4 kV
Power	30 kW
Switching frequency	75 kHz
Filter inductance (L_f)	14 mH
Line resistance (R_f)	0.1 ohm
DC link capacitor (C_{dc})	0.3 mF

Table 1: Designed System Parameters

1.2 Controller Design

The control scheme used for grid-connected operation is shown in Fig. 3. Synchronous reference frame-based vector control is the basic control scheme used for the 3 Level NPC converter. Grid voltage is used as the reference vector as shown in Fig. 3. All the sensed three phase variables are converted to the equivalent synchronous dq reference frame variables using wt.

In the synchronous reference frame, the fundamental component of all the variables behaves like dc parameters. For fundamental component control, there are three PI controllers used in the system—one voltage controller forming the slow acting outer control loop and two current controllers; one each in the d-axis and q-axis forming the higher bandwidth inner control loops. Feed-forward terms are used for decoupling the two current controller dynamics. The voltage controller regulates the MV dc bus voltage (V_{dc}) to the reference value (V_{dc}^*) and generates the reference(i_d^*) for the d-axis current controller. The d-axis current controller regulates

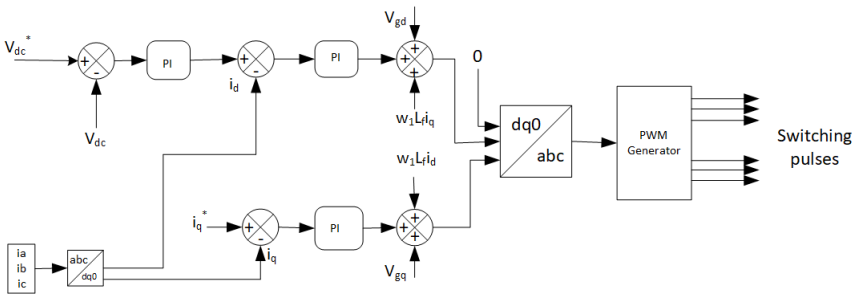

Figure 3: Control Scheme for AC-DC converter

the active component (i_d) of the fundamental grid current to this reference and generates the d-axis voltage component of the converter voltage (v_d). The objective of the q-axis current controller is power factor (pf) control on the grid side. The q-axis current controller regulates the reactive component (i_q) of the fundamental grid current to its reference (i_q) and generates the q-axis voltage component of the converter voltage (V_q). Unity power factor (UPF) is achieved by keeping $i_q = 0$. Hence, the controllers ensure that the error signals V_{dC}^e,i_d^e and i_q^e are regulated to zero. Fundamental three-phase modulating signals (m_a, m_b, m_c) are calculated from v_d, v_q .

Equation (1) gives the plant model $G_p(s)$ of the converter. At 75 kHz switching frequency, T_{sw} =13.3 μs. For the L-filter of $L_f = 14mH$and considering $R_f = 0.1$ ohm, $T_f = 200ms$.The inner current control loop has to be made as fast as possible. It is possible to select 1 kHz ($w_i = 2 * pi * 1000rad/s$) bandwidth for this controller because of 75 kHz switching frequency. By canceling the dominant pole ($1/T_f$) in the system with the zero ($1/T_c$) of the current controller as shown in (2), the current loop becomes a first-order system.This results in very good transient response for the current control loop. The open-loop transfer function $G_c - OL(s)$ for the current control is given in (3), where K_c is the gain of the current controller and is calculated from (4) for the required bandwidth w_i. The first order closed-loop current control transfer function $G_c - CL(s)$ is given in (5). In all these derivations, feed-forward terms are assumed to decouple the d- and q-axis[1].

$$G_p(s) = \frac{1}{R_f}(\frac{1}{1+sT_f}) = \frac{i_d}{v_d} = \frac{i_q}{v_q} \tag{1}$$

$$T_c = T_f = \frac{L_f}{R_f} \tag{2}$$

$$G_{c-OL}(s) = \frac{K_c}{sL_f} = \frac{i_d}{i_d} = \frac{i_q}{i_q^e} \tag{3}$$

$$K_c = w_i * L_f \tag{4}$$

$$G_{c-CL}(s) = \frac{1}{1+\frac{s}{w_i}} = \frac{i_d}{i_d^*} = \frac{i_q}{i_q^*} \tag{5}$$

Outer voltage control is designed from [3]

$$K_v = \frac{3}{2}\frac{C_d * w_v}{m}$$

$$K_v = 0.673$$

$$and\ K_i = 5.6$$

Parameter	Value
T_f	0.14
T_C	0.14
w_i	7500 rad/sec
K_c	660
f_{sw}	75 kHz

Table 2: Controller Parameters of Inner Current Loop

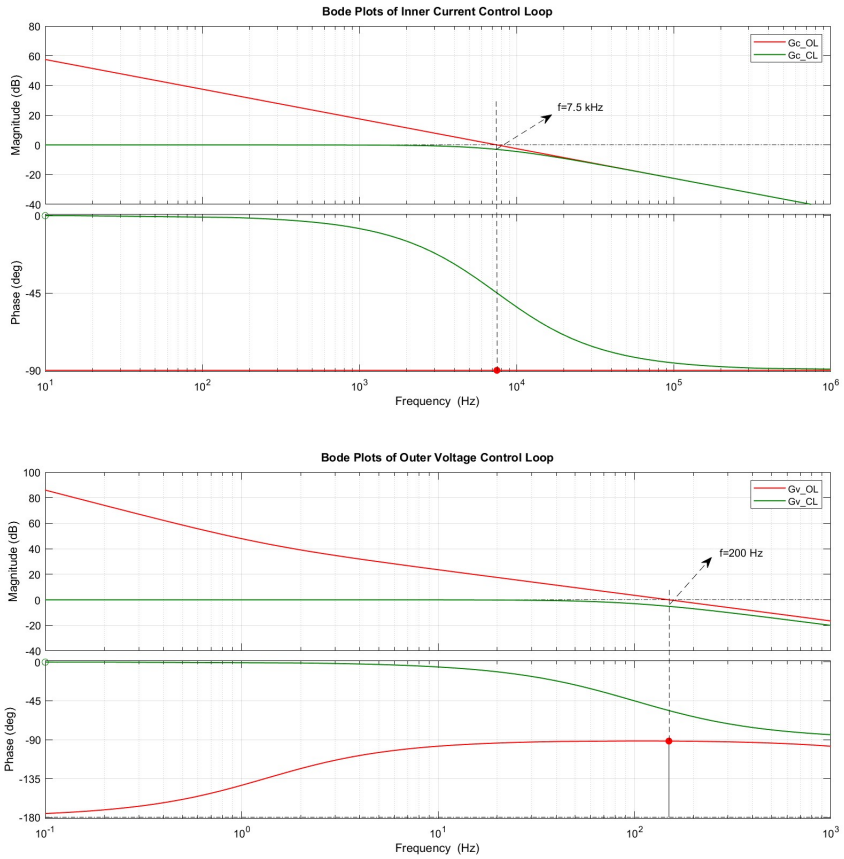

Figure 4: Bode Plots of the Control Transfer Functions.

2 DC-DC Converter Design

2.1 Power Circuit Design

Dual active bridge (DAB) converters are widely used in the applications requiring bidirectional power transmission, such as dc micro grid, electric vehicles and uninterruptible power supplies.The power circuit of the DC-DC DAB converter system is shown in Fig. 5.
Expression for inductor is given by

$$L = \frac{N_1}{N_2}\left(\frac{V_{dc1} * V_{dc2}}{2 * f_{swi} * P}\right)D(1-D)$$

$$L_{max} = 0.017066H$$

We take,

$$L = 10mH$$

Now,we put this value of L and then we get

$$D = 0.177$$

Expression for capacitor is given by

$$C = \frac{N_1}{N_2}\left(\frac{V_{dc1} + (\frac{N_1}{N_2})V_{dc2}}{2 * f_{swi} * L}\right)\frac{T_s}{2 * \triangle V}$$

$$= 1.51mF$$

Expression for phase shift is given by

$$\phi = \frac{D * T_{swi}}{2}$$

$$= 31.86degrees$$

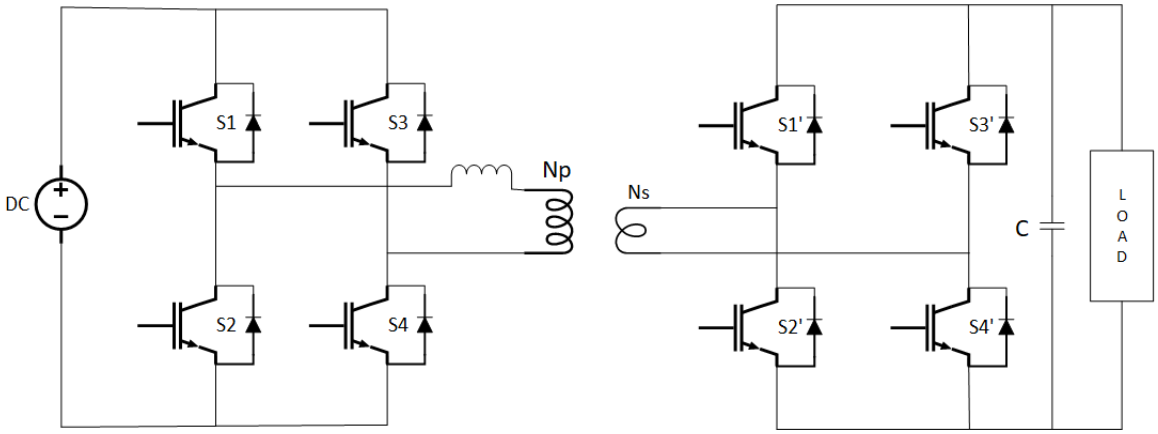

Figure 5: Circuit Diagram of DC-DC DAB Converter

2.2 Controller Design

The transfer function output current to phase shift $G_{io\phi}(s)$ is

$$G_{io\phi}(s) = \frac{\hat{i_0}}{\hat{\phi}} = V_g * \frac{8}{\pi^2}\left(\frac{sin\phi * s + \omega_s * cos\phi}{Ls^2 + \omega_s^2 * L}\right)$$

The transfer function output voltage to phase shift $G_{vo\phi}(s)$ is

$$G_{vo\phi}(s) = \frac{\hat{v_0}}{\hat{\phi}} = V_g * \frac{8}{\pi^2}\left(\frac{sin\phi * s + \omega_s * cos\phi}{C_0Ls^3 + \frac{L}{R_L}s^2 + (\omega_s^2 * LC_0 + \frac{8}{\pi^2})s + \frac{\omega_s^2 * L}{R_L}}\right)$$

The values of K_p and K_i for current controller are 0.1585 and 1759.8 respectively and for voltage controller are 0.04665 and 0.778 respectively.

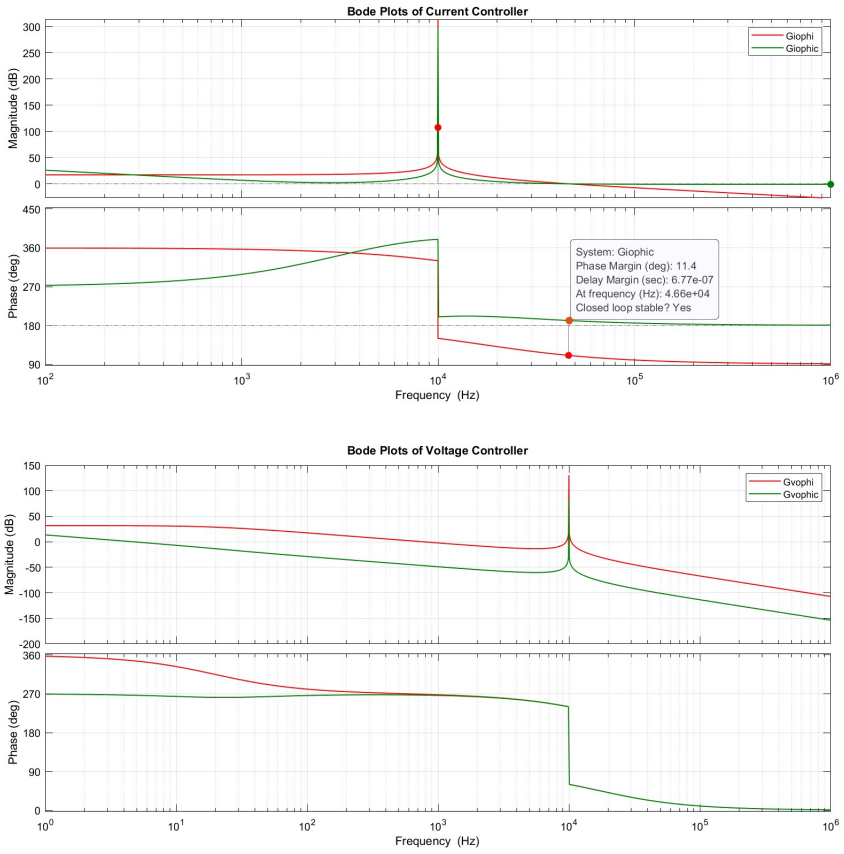

Figure 6: Bode Plot of DAB converter

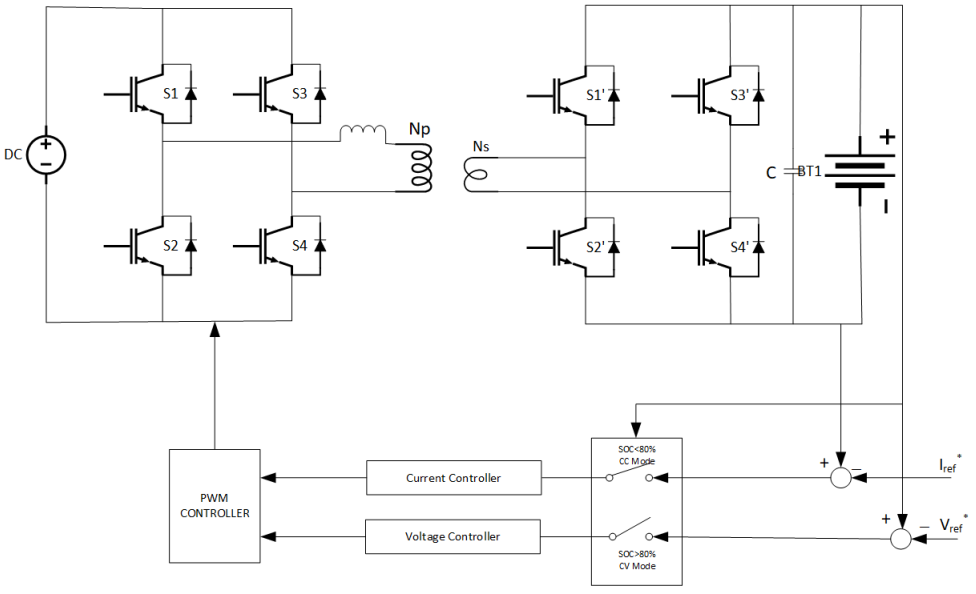

Figure 7: Control Scheme for DC-DC DAB Converter

Simulation Result

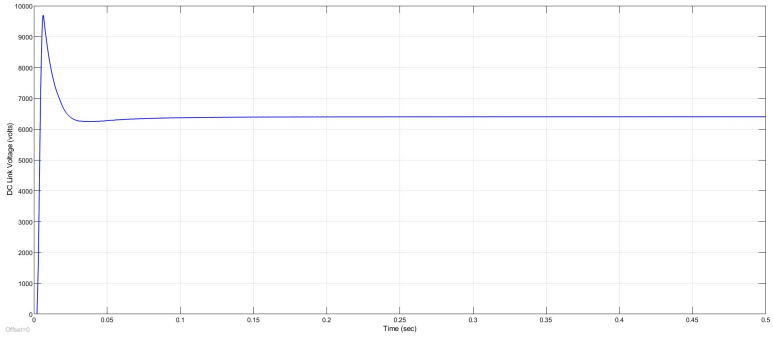

Figure 8: Waveform of DC link voltage

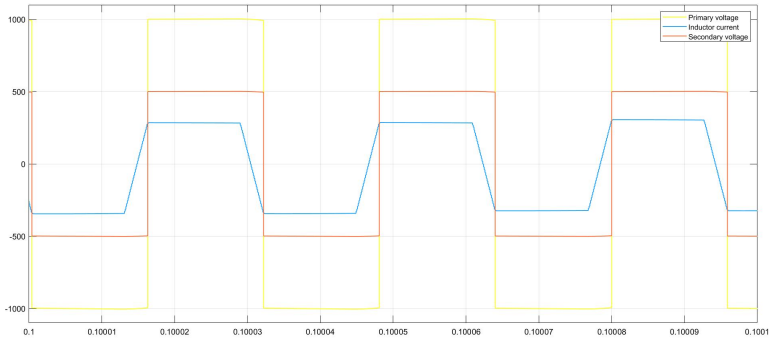

Figure 9: Waveform of DAB Converter

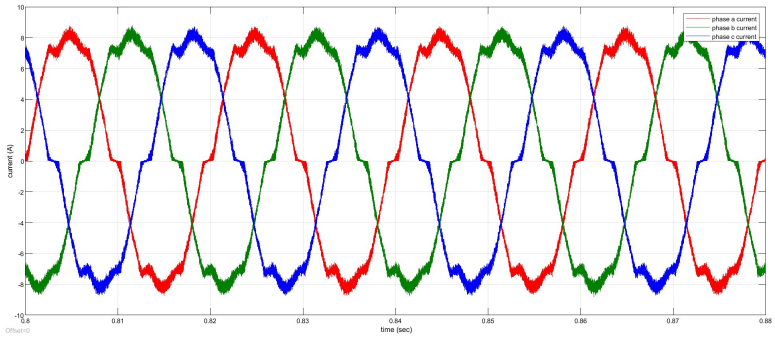

Figure 10: Waveform of Input Current

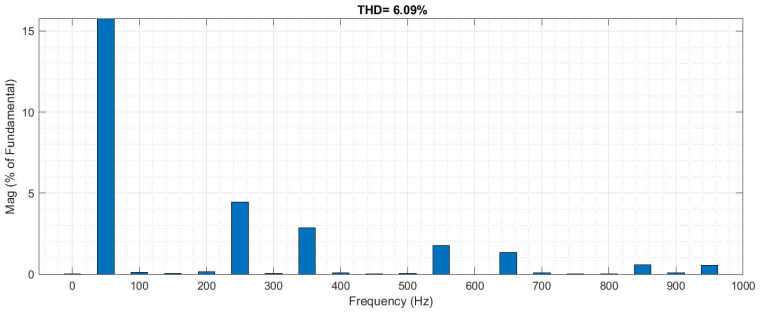

Figure 11: Input Grid Current FFT Analysis

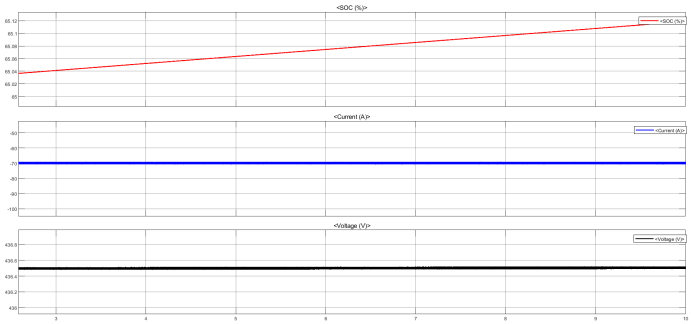

Figure 12: Waveform of Constant Current Charging

Conclusion

Firstly, design of each converter is done individually and then open loop simulations are performed and results are noted. Then modelling of AC-DC converter is done in synchronous frame of reference and controllers are designed using bode plots. The modelling of DC-DC converter is done using phasor transformations from [2]. The entire system simulations are performed and Constant current-Constant voltage charging is done for a battery of 400V,70 kWhr . All the simulations are performed in MATLAB and results are provided in the simulation results section.

REFERENCES

[1] S. Madhusoodhanan et al., "Harmonic Analysis and Controller Design of 15 kV SiC IGBT-Based Medium-Voltage Grid-Connected Three-Phase Three-Level NPC Converter," in IEEE Transactions on Power Electronics, vol. 32, no. 5, pp. 3355-3369, May 2017, doi: 10.1109/TPEL.2016.2582803.
[2] W. Han and L. Corradini, "Analytical Small-Signal Transfer Functions for Phase Shift Modulated Dual Active Bridge Converters Using Phasor Transformation," 2018 IEEE Energy Conversion Congress and Exposition (ECCE), 2018, pp. 1442-1448, doi: 10.1109/ECCE.2018.8558437.
[3] Setiawan, Iwan,Facta,Mochammad, Ardyono Priyadi, and Mauridhi Hery Purnomo. "Investigation of Symmetrical Optimum PI Controller based on Plant and Feedback Linearization in Grid-Tie Inverter Systems" International Journal of Renewable Energy Research-IJRER, Vol 7, No 3 (2017).